doi:10.1093/brain/awh485 *Brain* (2005), **128,** 1605–1612

Voxel-wise analysis of [^{123}I]β-CIT SPECT differentiates the Parkinson variant of multiple system atrophy from idiopathic Parkinson's disease

Christoph Scherfler,[1,*] Klaus Seppi,[1,*] Eveline Donnemiller,[2] Georg Goebel,[3] Christian Brenneis,[1] Irene Virgolini,[2] Gregor K. Wenning[1] and Werner Poewe[1]

Departments of [1]Neurology, [2]Nuclear Medicine and [3]Medical Statistics, Informatics and Health Economics, Innsbruck Medical University, Anichstrasse 35, 6020 Innsbruck, Austria

Correspondence to: Dr. Christoph Scherfler, Department of Neurology, Innsbruck Medical University, Anichstrasse 35, 6020 Innsbruck, Austria
E-mail: christoph.scherfler@uibk.ac.at
*These authors contributed equally to this work

To investigate the cerebral dopamine transporter status in the early stages of the parkinson-variant of multiple system atrophy (MSA-P), 15 patients with MSA-P and a disease duration up to 3 years were studied with [^{123}I]β-CIT single photon emission computed tomography (SPECT). Data were compared with 13 age-matched healthy control subjects and 15 patients with idiopathic Parkinson's disease (IPD), matched for age and disease duration. Parametric SPECT images of the specific-to-nondisplaceable equilibrium partition coefficient (V_3''), which is proportional to the receptor density (B_{max}) have been generated. To objectively localize focal changes in dopaminergic function throughout the entire brain volume without having to make an a priori hypothesis as to their location, statistical parametric mapping (SPM) was applied to our [^{123}I]β-CIT SPECT study. Both MSA-P and IPD patients showed significant decreases in striatal [^{123}I]β-CIT SPECT uptake. However, in MSA-P patients an additional reduction in midbrain [^{123}I]β-CIT signal was localized with SPM compared with control subjects (MSA-P, V_3'': 0.89 ± 0.37 versus controls V_3'': 1.81 ± 0.38; $P < 0.001$) and patients with IPD (V_3'': 1.84 ± 0.26; $P < 0.001$). Stepwise linear discriminant analysis of mean [^{123}I]β-CIT uptake in the putamen, caudate and midbrain identified the caudate and midbrain as indices to classify correctly 95.2% of subjects as either normal, patients with MSA-P or IPD. Voxel-wise analysis of [^{123}I]β-CIT SPECT revealed more widespread decline of monoaminergic transporter availability in MSA-P compared with IPD, matching the underlying pathological features. We suggest that the quantification of midbrain DAT signal should be included in the routine clinical analysis of [^{123}I]β-CIT SPECT in patients with uncertain parkinsonism.

Keywords: [^{123}I]β-CIT SPECT; multiple system atrophy; idiopathic Parkinson's disease; statistical parametric mapping; discriminant analysis

Abbreviations: AI = asymmetry index; [^{123}I]β-CIT = [^{123}I]-2β-carbomethoxy-3β-(4-iodophenyl)tropane; CI = confidence interval; DAT = dopamine transporter; FDG = fluorodesoxyglucose; FWHM = full width at half maximum; H&Y = Hoehn and Yahr; IPD = idiopathic Parkinson's disease; MNI = Montreal Neurological Institute; MSA-P = parkinsonian-variant of MSA; NAT = noradrenergic transporter; PET = positron emission tomography; ROI = region of interest; SERT = serotonin transporter; SPECT = single photon emission computed tomography; SPM = statistical parametric mapping; UPDRS = Unified Parkinson's Disease Rating Scale; V_3'' = specific-to-nondisplaceable equilibrium partition coefficient

Received October 18, 2004. Revised January 24, 2005. Accepted February 21, 2005. Advance Access publication April 7, 2005

Introduction

The development of radioligands to visualize the dopaminergic system with either single photon emission computed tomography (SPECT) or positron emission tomography (PET) led to a variety of studies aiming to characterize and discriminate disease entities presenting clinically with parkinsonism. Localization of either dopa decarboxylase activity by

[^{18}F]fluorodopa PET (Garnett *et al.*, 1983; Brooks *et al.*, 1990) and dopamine transporter (DAT) uptake as measured by a variety of DAT ligands for SPECT and PET (for a review, see Eckert and Eidelberg, 2004) has so far been based on the assessment of regions of interest (ROIs) outlining the caudate and putamen known to be affected most in idiopathic Parkinson's disease (IPD) and related disorders such as the parkinson-variant of multiple system atrophy (MSA-P), progressive supranuclear palsy or corticobasal degeneration. However, since striatal dopaminergic terminals are affected in all of those disease entities, evaluation of DAT binding or dopa decarboxylase activity by the ROI approach has limited value in discriminating between patients with IPD and atypical parkinsonian disorders (Brooks *et al.*, 1990; Pirker *et al.*, 2000*a*; Varrone *et al.*, 2001). However, [^{18}F]fluorodopa or DAT ligand uptake is not restricted to the striatum only. By applying statistical parametric mapping (SPM) to [^{18}F]fluorodopa PET studies (a technique that objectively localizes focal changes of the radiotracer throughout the entire brain volume without having to make an a priori hypothesis as to their location), several research groups were able to identify distinct alterations of the dopa decarboxylase activity in other brain regions than the striatum in different stages of IPD and related disorders (Rakshi *et al.*, 1999; Whone *et al.*, 2003; Scherfler *et al.*, 2004).

The radiotracer [^{123}I]-2β-carbomethoxy-3β-(4-iodophenyl)tropane ([^{123}I]β-CIT), a cocaine derivative with a high-affinity for dopamine and serotonin transporters (SERT) was reported to be a sensitive marker of disease progression in parkinsonian disorders and was shown to correlate well with disease disability rated by the Hoehn and Yahr (H&Y) scale (Hoehn and Yahr, 1967) and the Unified Parkinson's Disease Rating Scale (UPDRS) (Fahn and Elton, 1987; Boja *et al.*, 1991; Neumeyer *et al.*, 1991; Seibyl *et al.*, 1995; Bruecke *et al.*, 1997; Pirker *et al.*, 2002).

In the present study we aimed to characterize the integrity of the dopaminergic system within the entire brain volume of patients with IPD and MSA-P with a maximum disease duration of 3 years using SPM and [^{123}I]β-CIT SPECT. Subsequently, brain regions of significant signal alterations have been subjected to a stepwise discriminant analysis in order to evaluate the potential of [^{123}I]β-CIT SPECT to classify correctly patients with MSA-P, IPD and healthy controls on an individual basis.

Material and methods

Subjects

Fifteen patients with MSA-P (seven females and eight males; mean age 61.8 ± 9.3 years) and 15 patients with IPD (five females and 10 males; mean age 61.3 ± 6.8 years) were recruited consecutively from referrals to the Movement Disorders Clinic at the Department of Neurology at Innsbruck Medical University. Only patients ranging between 50 and 70 years of age with clinically probable disease according to established diagnostic criteria and a disease duration not exceeding 3 years were eligible for the study (Hughes *et al.*, 1992; Gilman *et al.*, 1998). At the time of the SPECT study, 12 of the MSA-P patients had been classified as 'probable', and three as 'possible' who were re-classified as 'probable' at a follow-up visit one year after the SPECT examination. In addition to [^{123}I]β-CIT SPECT brain MRI was performed to exclude those with severe white matter, vascular or space-occupying lesions within the cerebrum.

Motor disability related to parkinsonism was assessed in all patients in off-drug states using part III of the UPDRS and classified according to H&Y. Signs of dementia, vertical gaze palsy or cerebellar signs were absent in all patients in the MSA-P cohort.

Disease duration ranged from 0.4 to 3 years (mean disease duration 2 ± 0.8 years). Mean UPDRS off motor score (part III) was 38.9 ± 10.7. Patients with IPD were matched for age and disease duration (mean disease duration 1.7 ± 0.8 years). Mean UPDRS off motor score (part III) was 21.5 ± 7.2. Seven patients with IPD and eight patients with MSA-P were receiving regular levodopa therapy. In addition, 11 of the IPD and five of the MSA-P patients were taking dopamine agonist medication. None of the patients was taking selective serotonin reuptake inhibitors.

[^{123}I]β-CIT SPECT findings for IPD and MSA-P cases were also compared with a group of 13 age-matched healthy control subjects (six females and seven males; mean age 61 ± 8.3 years). The group of healthy controls consisted of five patients with peripheral neurological disorders (sensorimotor polyneuropathy in three cases and radial nerve pressure palsies in two cases) and eight healthy volunteers without evidence of neurological disease.

The study was approved by the Ethics Committee of the Innsbruck Medical University. Subjects' consent was obtained according to the Declaration of Helsinki.

Radiopharmaceutical preparation

[^{123}I]β-CIT was obtained from the Austrian Research Centre, Seibersdorf. Radiolabelling, radiochemical purity, radiopharmaceutical safety and dosimetry of the tracers have been described previously (Kuikka *et al.*, 1994).

Scanning protocol

After blocking thyroid uptake with 600 mg sodium perchlorate orally 30 min before tracer application, patients and controls received a bolus dose of 148–185 MBq [^{123}I]β-CIT intravenously. The patient's head was positioned in a head holder by means of a crossed laser beam system. Data acquisition started 18 h post tracer application and lasted 42 min and 40 s (Laruelle *et al.*, 1994). All scans were performed with a dual-detector scintillation camera ADAC, Vertex-Plus (EPIC detector system, VXHR collimator) with a spatial resolution of 12 mm full width at half maximum (FWHM) in the transaxial plane. Camera heads were equipped with medium-energy collimators. For each scan a total of 64 projections (80 s per frame) were collected in a step-and-shoot mode. The image data were reconstructed by standard filtered backprojection using a Gaussian-weighted Ramp filter (cut-off frequency 0.38 Nq) and attenuation was corrected using Chang's first-order method (attenuation coefficient $\mu = 0.12$ cm^{-1}).

Data analysis

The irreversible binding characteristics and the stability of regional [^{123}I]β-CIT uptake 18 h post application was shown to allow estimation of the specific-to-nondisplaceable equilibrium partition coefficient (V_3''), which is proportional to the receptor density (B_{max}) (Laruelle *et al.*, 1994). V_3'' can be calculated according to the

equilibrium model introduced by Laruelle *et al.* (1994). Under equilibrium conditions between a compartment with specific binding and a compartment representing nonspecifically bound and free activity, V_3'' was shown to be proportional to B_{max} given that both the dissociation constant and the volume of distribution of the nonspecifically bound and free activity compartment (V_2) is relatively invariant in the population.

By assuming that the occipital region is devoid of dopamine transporters, the parameter V_3'' can be computed for every voxel using the formula:

$$\frac{(\text{counts per minute/voxel})_{V_T} - (\text{counts per minute/voxel})_{V2}}{(\text{counts per minute/voxel})_{V2}}$$

where V_T represents the specific, the nonspecifically bound and the free activity compartment.

Two methods of analysis were employed: (i) a ROI approach; and (ii) SPM. This allowed exploratory voxel-by-voxel group comparisons throughout the entire brain volume without requiring an a priori hypothesis. Analysis of data was performed on a Windows XP workstation (Pentium 4, Sony PCV-RS404). Image transformation, computation of V_3'' and statistical analysis was performed using SPM2 (Wellcome Department of Cognitive Neurology, London, UK; Friston *et al.*, 1995) implemented in Matlab 5.3 (Mathsworks Inc., Sherborn, MA, USA). V_2 was estimated by placing a circular ROI (diameter 32 mm) on four consecutive transversal slices within each occipital lobe.

Calculation of ROIs

Four ROIs were outlined by inspection of integrated transversal [^{123}I]β-CIT SPECT images using the software package MRICro 1.37 (Chris Rorden, University of Nottingham, Nottingham, UK). These included the head of the caudate nucleus (circle, diameter 10 mm), and the putamen (two circles, diameter 10 mm each). Caudate and putaminal asymmetry indices (AIs) were calculated, reflecting the percentage difference between the SPECT signal in the respective region of higher tracer uptake compared with the contralateral region using the following formula:

$$\text{AI} = \frac{(\text{higher SPECT signal} - \text{lower SPECT signal})}{(\text{higher SPECT signal}) \times 100}.$$

Additionally, the hemispheric ratio between the caudate and putaminal SPECT signal was measured. Right and left caudate and putaminal [^{123}I]β-CIT uptake was averaged for each subject to allow for statistical analysis.

SPM analysis

As there is insufficient anatomical detail in parametric images of [^{123}I]β-CIT V_3'', an indirect approach introduced by Rakshi *et al.* (1999) for [^{18}F]fluorodopa PET images was employed to achieve accurate spatial normalization. Since a [^{123}I]β-CIT raw data image and a summed [^{18}F]fluorodopa PET image provide similar anatomical information, the raw data [^{123}I]β-CIT image of each control subject was normalized onto the [^{18}F]fluorodopa PET template in MNI (Montreal Neurological Institute) space (Scherfler *et al.*, 2004). A mean image of the previously normalized raw data [^{123}I]β-CIT acquisitions was then computed and used as a template image. For each individual SPECT acquisition, a parametric V_3'' image was calculated. The raw data image was transformed onto the [^{123}I]β-CIT template image and the resulting transformation parameters were then applied to the corresponding subject's parametric V_3'' image. Spatial normalization works by minimizing the sum of squared difference between raw data [^{123}I]β-CIT image and the [^{123}I]β-CIT template. The algorithm comprises a 12-parameter affine transformation of the raw data [^{123}I]β-CIT image onto the [^{123}I]β-CIT template image followed by estimating the nonlinear deformations between the applied images. A gaussian kernel ($6 \times 6 \times 6$ mm) was then convolved with the spatially normalized parametric images to smooth them in order to accommodate interindividual anatomic variability and to improve signal-to-noise for the statistical analysis.

Parametric images transformed into MNI space enable comparisons across study groups in analogous voxel regions of the brain volume. Since DAT densities are known to be low in the occipital lobe and the cerebellum, a brain mask for those areas was created in order to minimize voxels of no-interest for multi-comparison corrections. A total of 61 744 voxels were analysed. The obtained datasets allowed for categorical comparisons of [^{123}I]β-CIT V_3'' values among the MSA-P, IPD and control groups. SPM maps surviving a threshold of $P < 0.001$ were further corrected for multiple comparisons. Data cluster revealed by SPM to show significant differences of V_3'' values between groups were transformed onto the individual V_3'' image to obtain mean regional uptake values.

One way analysis of variance (ANOVA) and post hoc least significance difference was applied for clinical data and mean ROI values. For multiple comparisons between groups, a Bonferroni correction was applied. To discriminate between groups, linear discriminant analysis was performed with a forward selection mechanism based on Wilks' lambda as selection criteria for potential predictors, i.e. [^{123}I]β-CIT V_3'' mean value of the caudate, the putamen and the midbrain as well as the ratio of caudate to putamen and the AI of the caudate and the putamen, respectively. An F-value of 3.84 and 2.71 was used for inclusion and removal of variables, respectively. For group membership, the same a priori probability was assumed for all cases.

For validation of the model we used a leave-one-out procedure. The cut-off value between two groups was determined as follows: (i) the mean and its confidence interval (CI) of both groups were calculated; and (ii) the cut-off value was determined by averaging over the lower bound of the CI of one group and the upper bound of the other group. Statistical analysis was carried out using a commercial software package (SPSS for Windows 8.0, SPSS UK, Surrey, UK).

Results

Patients (Table 1)

Patients groups and control subjects were matched for age. Maximum disease duration was limited by 3 years and was not significantly different between MSA-P and IPD patients.

However, when compared with IPD patients, the UPDRS motor score was significantly more affected in MSA-P patients ($P < 0.001$), whereas no significant difference between patient groups was apparent for H&Y rating.

ROI analysis of [^{123}I]β-CIT SPECT

Regional mean [^{123}I]β-CIT V_3'' values of the study groups and the intergroup statistics are detailed in Table 2. One-way ANOVA showed a significant decrease of caudate and putamen [^{123}I]β-CIT uptake in MSA-P ($P < 0.001$) and IPD

Table 1 Demographic and clinical characteristics of patients with MSA-P, IPD and control subjects

	Age (years)	Sex (M/F)	Disease duration (years)	H&Y stage	UPDRS motor score
MSA-P ($n = 15$)					
Mean ± SD	61.8 ± 9.3	8/7	2 ± 0.8	2.6 ± 0.7	38.9 ± 10.7*
IPD ($n = 15$)					
Mean ± SD	61.3 ± 6.8	10/5	1.7 ± 0.8	1.9 ± 0.9	21.5 ± 7.2
Controls ($n = 13$)					
Mean ± SD	61 ± 8.3	7/6			

Values represent the means (±1 SD). Intergroup differences were calculated by one-way ANOVA with *post hoc* least statistical significance correction. *$P < 0.001$ versus IPD patients.

Table 2 Mean regional putamen and caudate [^{123}I]β-CIT V_3'' in MSA-P, IPD and control subjects

	Caudate	Putamen	AI (%) caudate	AI (%) putamen	Ratio caudate/putamen
MSA-P ($n = 15$)					
Mean ± SD	5.23*** ± 2.25	5.93*** ± 2.64	12.1** ± 11.5	15.4*** ± 12.2	0.87† ± 0.07
IPD ($n = 15$)					
Mean ± SD	5.81*** ± 1.33	6.13*** ± 1.44	10.6* ± 7.6	10.1 ± 8.6	0.95 ± 0.09
Controls ($n = 13$)					
Mean ± SD	9.1 ± 1.8	9.7 ± 1.8	3.7 ± 3.6	4 ± 2.3	0.93 ± 0.04

Values represent the means (±1 SD). Intergroup differences were calculated by one-way ANOVA with *post hoc* least statistical significance correction. *$P < 0.05$, **$P < 0.01$, ***$P < 0.001$ versus normal controls, respectively. $^{\dagger}P < 0.01$ versus IPD patients.

($P < 0.001$) patients versus normal control subjects. MSA-P and IPD patients had similar levels of striatal [^{123}I]β-CIT uptake. Comparing patient groups with the normal control group, the AI of [^{123}I]β-CIT uptake was significantly increased in the caudate (MSA-P group, $P < 0.01$; IPD group $P < 0.05$) and putamen (MSA-P group, $P < 0.001$). The putaminal AI of IPD patients was altered compared with normal control subjects, but no significant difference was evident. Furthermore, no significant difference in caudate and putaminal [^{123}I]β-CIT asymmetry was found between MSA-P and IPD patients. The caudate-to-putamen ratio of [^{123}I]β-CIT V_3'' was significantly decreased in MSA-P patients ($P < 0.01$) compared with IPD and control subjects.

[^{123}I]β-CIT SPECT SPM findings (Table 3)

SPM of parametric [^{123}I]β-CIT V_3'' images confirmed the results of striatal ROI analysis. Additionally, significant relative decreases of V_3'' values were localized in the ventral and dorsal midbrain and in the pons in MSA-P patients (areas of the red nucleus, substantia nigra and raphe nuclei) compared with IPD patients. No significant increases in [^{123}I]β-CIT V_3'' values were detected in the MSA-P group versus the IPD and control group (Figure 1). Compared with control subjects, significant reductions of [^{123}I]β-CIT signal were localized in the caudate and putamen in both patient groups, whereas significant decreases in the dorsal and ventral midbrain [^{123}I]β-CIT V_3'' values were observed only in the MSA-P group.

Respective calculation of mean [^{123}I]β-CIT uptake in the midbrain cluster showed mean V_3'' values of 0.89 ± 0.37 in MSA-P, 1.84 ± 0.26 in IPD, and 1.81 ± 0.38 in control subjects.

Discrimination among control subjects, IPD and MSA-P (Table 4)

Stepwise linear discriminant analysis including caudate, putamen, midbrain mean V_3'' values, the caudate-to-putamen ratio and the AI of the caudate and putamen were applied to predict the clinical diagnosis. Two variables (the caudate and midbrain mean V_3'' values) appeared in the final model. The sensitivity of this mathematical model, which used a linear function including the regional [^{123}I]β-CIT V_3'' mean values of the abovementioned structures, was assessed by calculating probability scores. Overall, 41 out of 43 subjects, i.e. 95.2% were classified correctly. There was a good discrimination of MSA-P patients, IPD and control subjects. None of the control subjects was wrongly classified into the patients groups. For both the IPD and the MSA cohort, 14 out of 15 patients were classified correctly into each group. On the other hand, only one MSA-P patient and one patient with IPD were classified wrongly into the other patient's group. The validation of the model by the leave-one-out procedure showed the same classification error as the training model (5%). Additionally, a discrimination pattern identical to that for the probability scores was obtained by applying cut-off values (caudate V_3'' value, 7.6 and midbrain V_3'' value, 1.4) to the dataset.

Discussion

This is the first DAT SPECT study to characterize, within the entire brain volume, abnormalities in DAT availability in a group of MSA-P and IPD patients. We have applied SPM to spatially normalized parametric images of [^{123}I]β-CIT V_3'' and

Table 3 Between-group SPM findings showing the locations of significant decreases of [^{123}I]β-CIT V_3'' values in MSA-P, IPD and control subjects

[^{123}I]β-CIT V_3'' Brodmann area	Talairach coordinates*			*Z* score	*P* values (corrected)	Height threshold
	x	*y*	*z*			
Decreases in MSA-P patients compared with IPD patients						
Dorsal midbrain	4	−26	−12	6.21	0.0001	0.001
Ventral midbrain	4	−10	−6	5.05	0.001	
Dorsal pons	0	−31	−22	4.15	0.0001	
Decreases in IPD patients compared with control subjects						
Right striatum (putamen)	28	0	−2	6.63	0.0001	0.001
Left striatum (putamen)	−24	−4	0	6.07	0.0001	
Right striatum (caudate)	12	20	3	5.31	0.0001	
Left striatum (caudate)	−12	21	1	4.56	0.01	
Decreases in MSA-P patients compared with control subjects						
Right striatum (putamen)	26	−6	−1	5.97	0.0001	0.001
Ventral midbrain	2	−10	−8	5.97	0.0001	
Left striatum (caudate)	−8	22	4	5.2	0.0001	
Left striatum (putamen)	−18	−2	−2	4.9	0.001	
Right striatum (caudate)	10	12	5	4.56	0.006	
Dorsal midbrain	4	−24	−12	4.25	0.021	
Pons	−4	−26	−26	4.15	0.03	

*MNI coordinates have been transformed to Talairach coordinates using the software package mni2tal.m (http: //www.mrc-cbu.cam.ac.uk/Imaging/Common/mnispace.shtml).

Table 4 Diagnostic classification matrix, based on regional [^{123}I]β-CIT uptake

Clinical classification	Predicted group by regional [^{123}I]β-CIT		
	Controls	IPD	MSA-P
Controls ($n = 13$)	**13 (100%)**	0	0
IPD ($n = 15$)	0	**14 (93.3%)**	1 (6.7%)
MSA-P ($n = 15$)	0	1 (6.7%)	**14 (93.3%)**

The classification of subjects' caudate and midbrain [^{123}I]β-CIT uptake with respect to their clinical diagnosis has been calculated by stepwise discriminant analysis. Rows represent the clinical diagnosis and columns the diagnosis predicted by regional [^{123}I]β-CIT V_3'' values. Bold indicates correct diagnosis.

localized similar reduction in striatal β-CIT V_3'' in early MSA-P and IPD to those detected using a standard ROI approach. SPM, however, enabled us to localize objectively focal β-CIT V_3'' changes in the midbrain and pontine regions in MSA-P which could not have been predicted by visual inspection or ROI analysis of [^{123}I]β-CIT SPECT images. The routine assessment of a [^{123}I]β-CIT SPECT image focuses primarily on the striatum as the brain area with the highest DAT uptake, whereas regions of the brain with somewhat lower but still detectable [^{123}I]β-CIT uptake might be neglected by the investigator, as not being properly visualized by most software packages for image analysis.

Another drawback when outlining brain volumes of small sizes as the ventral and dorsal midbrain is the limited anatomical information provided by [^{123}I]β-CIT SPECT, forcing the investigator to generate an a priori assumption on the size and shape of the region to be evaluated. In contrast, no a priori hypothesis regarding the localization of SPECT signal is required by SPM, assuming that the spatial normalization of [^{123}I]β-CIT SPECT V_3'' images onto the MNI space was precise. It is possible that the relative differences in contrast and intensity between [^{123}I]β-CIT mean images and the individual [^{123}I]β-CIT SPECT of a patient with low DAT availability might affect spatial normalization. The normalization process is partly dependent on these factors, but the degree to which it might be affected will also depend on the particular constraints of the normalization algorithm (see Methods). If the spatial normalization had been imprecise, this would have represented a substantial source of error variance and we would not have obtained high *Z* scores for [^{123}I]β-CIT V_3'' changes in the patients' groups. Accurate spatial normalization is further supported by the SPM maps being accurately rendered onto the striatal and midbrain regions of the standard normalized MRI, with the maximal scores identified in MNI space corresponding to striatal and midbrain structures, as verified by visual inspection.

The midbrain area of reduced [^{123}I]β-CIT uptake in the MSA-P cohort identified by SPM comprises a volume of about 5000 mm^3 and showed the highest *Z* scores in the dorsal areas. In the midbrain, [^{123}I]β-CIT has been shown to be taken up by SERT, DAT and noradrenergic transporters (NATs) (Innis *et al.*, 1991; Uhl, 1992; Staley *et al.*, 1994; Pirker *et al.*, 2000*b*). Peak [^{123}I]β-CIT uptake in the midbrain occurs 4 h after injection, and a stable state of transient equilibrium has been suggested to be reached between 20 and 24 h for both the SERT and DAT system (Pirker *et al.*, 2000*b*). Although a precise assignment of the [^{123}I]β-CIT signal loss in the

midbrain is restricted by the non-selective tracer-to-receptor binding and the limited spatial resolution of about 10 mm FWHM, there is evidence that the [^{123}I]β-CIT uptake is predominately to SERT in that distinct region of the brain. In an autoradiographical study of post mortem human brain, Staley *et al.* (1994) showed that [^{125}I]β-CIT binding in the thalamus, hypothalamus and midbrain (with the exception of the substantia nigra) was completely displaced by addition of the selective serotonin reuptake inhibitor, citalopram. Further, Pirker *et al.* (1995) found evidence of a reduction in midbrain [^{123}I]β-CIT binding in a group of depressed patients treated with citalopram compared with a group of healthy volunteers. Consequently, the reduced [^{123}I]β-CIT uptake detected with SPECT in the dorsal and ventral midbrain of the MSA-P group may imply a widespread decline of primarily the SERT system compared with IPD, even though potential alterations of the DAT and NAT system cannot be excluded. This would be in line with reported neuropathological findings in MSA-P patients, showing neuronal loss in brainstem areas containing DAT, SERT or NAT bearing neurons as the substantia nigra, the locus coeruleus and the raphe nuclei (Wenning *et al.*, 1997, 2004; Papp and Lantos, 1994).

To estimate the degree of SERT dysfunction in MSA, further imaging studies are needed, applying selective radioligands for the SERT (for a review, see Hesse *et al.*, 2004).

In addition, SPM interrogation revealed a severe decline in caudate and putaminal [^{123}I]β-CIT uptake in the patient groups compared with healthy controls. This is in line with previous studies using the ROI technique (Bruecke *et al.*, 1997; Pirker *et al.*, 2000*a*; Varrone *et al.*, 2001). The domain of [^{123}I]β-CIT SPECT has so far been the quantification of striatal DAT uptake allowing to differentiate between movement disorders associated with dopaminergic degeneration and those which are not (Poewe and Scherfler, 2003). Hence, [^{123}I]β-CIT SPECT is widely employed in a clinical setting to support diagnostic processes in a number of different parkinsonian syndromes relating to isolated tremor symptoms not fulfilling essential tremor criteria, drug-induced parkinsonism or psychogenic parkinsonism which cannot reliably be separated on clinical grounds. However, the evaluation of striatal DAT uptake by the ROI approach has been reported so far to have no potential in differentiating early MSA-P from IPD patients (Pirker *et al.*, 2000). By applying SPM to our dataset, a significant reduction of midbrain and pons [^{123}I]β-CIT availability in MSA-P patients but not in patients with IPD was detected. Further stepwise discrimination analysis revealed that 95.2% (i.e. 41 out of 43 subjects) could be correctly classified as either normal, patients with IPD or patients with MSA-P when considering the caudate and brainstem [^{123}I]β-CIT signal in the image analysis. To discriminate between the patients' groups and the healthy control group, the caudate V_3'' value emerged as slightly superior (Wilks' lambda = 0.33) compared with the putaminal V_3'' value (Wilks' lambda = 0.37), which might not have been not suspected for IPD versus control subjects.

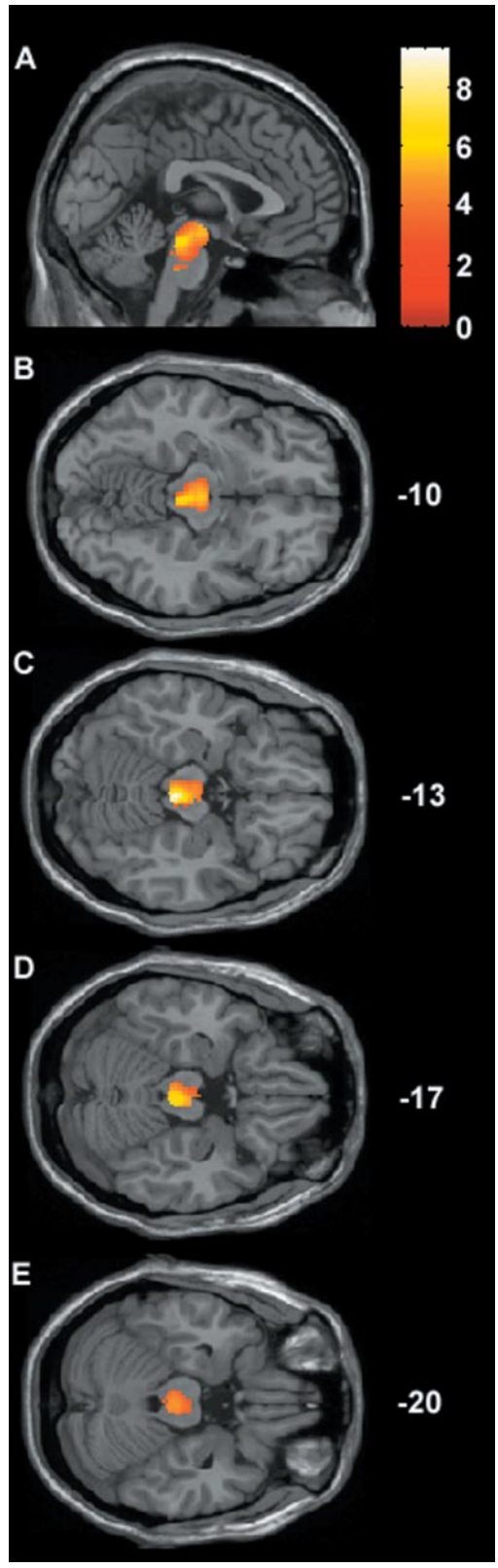

Fig. 1 SPM{Z} Sagital (**A**) and transverse maximum intensity projection maps rendered on to a stereotactically normalized MRI scan, showing areas of significant decreases in midbrain (**B**,**C**) and pons (**D**,**E**) [^{123}I]β-CIT V_3'' values in MSA-P compared with IPD. Numbers in B to E correspond to the z coordinate in Talairach space.

Considering the limited spatial resolution of a conventional dual-headed SPECT camera, partial volume effects are likely to occur, affecting particularly the quantification of signals in structures smaller than twice the FWHM resolution of the scanner used. This nonlinear effect leads to an underestimation of the radioactivity concentration in small objects (Glover and Pelc, 1979; Hoffman *et al.*, 1979; Kojima *et al.*, 1989). In the present study in particular the posterior parts of the putamen are likely to be affected, resulting in a slightly underestimated β-CIT signal in subjects with relatively high putaminal tracer uptake, which might contribute to the somewhat weaker classification index of the putaminal β-CIT signal. On the other hand, spill-over effects occur from areas with higher [^{123}I]β-CIT uptake into adjacent brain areas, as it is the case between the caudate and anterior putamen, leading to an overestimation of the [^{123}I]β-CIT uptake in the caudate of subjects with high putaminal signal. Since the potential to discriminate between patients and healthy controls is similar between the caudate and putaminal predictor and is likely to be enhanced for the latter by increasing the spatial resolution of the SPECT camera, both brain regions should be taken into account for the classification of subjects.

In the past a considerable number of either radiotracer-based or MRI-based image studies attempted to describe distinct patterns specific for MSA-P or IPD. None of those studies applied both a voxel-based approach in order to identify signal alterations in brain regions of IPD and MSA-P patients and a further discriminant analysis to search for indices with the potential to assign correctly individual patients to their parkinsonian illness. Hence, no comparisons between outcome measures of the voxel-wise analysis of our [^{123}I]β-CIT SPECT data and other imaging paradigms can yet be made. Classifications of high accuracy for patients with MSA-P and IPD have been reported for ROI analysis of both MRI-based techniques such as diffusion weighted imaging, magnetic transfer imaging and MRI volumetry (Schulz *et al.*, 1999; Eckert *et al.*, 2004; Schocke *et al.*, 2004) and radiotracer based methods such as [^{11}C]raclopride and [^{18}F]fluorodeoxyglucose (FDG) PET (Antonini *et al.*, 1997) as well as for [^{123}I]iodobenzamide and cardiac [^{123}I]metaiodobenzylguanidine SPECT (Schulz *et al.*, 1994; Braune *et al.*, 1999). Voxel-wise approaches of MRI volumetry, [Tc^{99m}]-ethylcysteine dimer SPECT and [^{18}F]FDG PET have so far reported significant alterations between groups of IPD and MSA-P patients (Brenneis *et al.*, 2003; Juh *et al.*, 2004; Van Laere *et al.*, 2004).

The results of our study underline the use of voxel-wise analysis as a first step in comparing patient groups, as this method is independent from a priori information on the size and localization of the imaging outcome measure. Once a brain region of significant signal alteration has been identified by SPM in a group of subjects, the region can be extracted and transformed onto an individual [^{123}I]β-CIT SPECT dataset for further ROI analysis. The application of SPM to our [^{123}I]β-CIT datasets revealed an area within the midbrain and pons of reduced radioligand uptake in patients with MSA-P. Adding the identified brainstem area to the routinely performed striatal ROI analysis indicated a high potential for [^{123}I]β-CIT SPECT to discriminate between IPD, MSA-P and controls. Considering the described brainstem area in the assessment of individual [^{123}I]β-CIT SPECT datasets will extend the application of [^{123}I]β-CIT SPECT as a powerful and widely available tool to improve the diagnostic accuracy of patients who present with diagnostic features of both MSA-P and IPD in their early disease stages. Further studies are needed to evaluate whether the application of the presented technique could be extended to patients with uncertain atypical parkinsonism other than MSA-P.

Acknowledgements

The study was supported by the Austrian Federal Ministry of Science and Transport (GZ 70038/2 PR 4/98).

References

Antonini A, Leenders KL, Vontobel P, Maguire RP, Missimer J, Psylla M, Gunther I. Complementary PET studies of striatal neuronal function in the differential diagnosis between multiple system atrophy and Parkinson's disease. Brain 1997; 120: 2187–95.

Boja JW, Patel A, Caroll FI, Rahman MA, Philip A, Lewin AH, et al. [125]-RTI55: a potent ligand for dopamine transporters. Eur J Pharmacol 1991; 194: 133–4.

Braune S, Reinhardt M, Schnitzer R, Riedel A, Lucking CH. Cardiac uptake of [123I]MIBG separates Parkinson's disease from multiple system atrophy. Neurology 1999; 53: 1020–5.

Brenneis C, Seppi K, Schocke MF, Muller J, Luginger E, Bosch S, et al. Voxel-based morphometry detects cortical atrophy in the Parkinson variant of multiple system atrophy. Mov Dis 2003; 18: 1132–8.

Brooks DJ, Ibanez V, Sawle GV, Quinn N, Lees AJ, Mathias CJ, et al. Differing patterns of striatal 18F-dopa uptake in Parkinson's disease, multiple system atrophy, and progressive supranuclear palsy. Ann Neurol 1990; 28: 547–55.

Bruecke T, Asenbaum S, Pirker W, Djamshidian S, Wenger S, Wober C, et al. Measurement of the dopaminergic degeneration in Parkinson's disease with [123I]beta-CIT and SPECT. Correlation with clinical findings and comparision with multiple system atrophy and progressive supranuclear palsy. J Neural Trans Suppl 1997; 50: 9–24.

Eckert T, Eidelberg D. The role of functional neuroimaging in the differential diagnosis of idiopathic Parkinson's disease and multiple system atrophy. Clin Auton Res 2004; 14: 84–91.

Eckert T, Sailer M, Kaufmann J, Schrader C, Peschel T, Bodammer N, et al. Differentiation of idiopathic Parkinson's disease, multiple system atrophy, progressive supranuclear palsy, and healthy controls using magnetization transfer imaging. NeuroImage 2004; 21: 229–35.

Fahn S, Elton RL, Members of the Unified Parkinson's Disease Rating Scale Development Committee. Unified Parkinson's disease rating scale. In: Fahn S, Marsden CD, Calne DB, Goldstein M, editors. Recent developments in Parkinson's disease. Vol. 2. Florham Park (NJ): Macmilian Healthcare Information; 1987. p. 153–64.

Friston KJ, Ashburner J, Frith CD, Poline JB, Heather JD, Frackowiak RS. Spatial registration and normalization of images. Hum Brain Mapp 1995; 3: 165–89.

Garnett ES, Firnau G, Nahmias C. Dopamine visualized in the basal ganglia of living man. Nature 1983; 305: 137–8.

Gilman S, Low P, Quinn N, Albanese A, Ben-Shlomo Y, Fowler C, et al. Consensus statement on the diagnosis of multiple system atrophy. American Autonomic Society and American Academy of Neurology. Clin Auton Res 1998; 8: 359–62.

Glover G, Pelc N. The nonlinear partial volume artefact. J Comput Assisted Tomogr 1979; 25: 79–86.

Hesse S, Henryk B, Schwarz J, Sabri O, Müller U. Advances in *in vivo* imaging of serotonergic neurons in neuropsychiatric disorders. Neurosci Biobehav Rev 2004; 28: 547–63.

Hoehn MM, Yahr MD. Parkinsonism: onset, progression and mortality. Neurology 1967; 17: 427–42.

Hoffman EJ, Huang SC, Phelps ME. Quantification in positron emission tomography. 1. Effect of object size. J Comput Assist Tomogr 1979; 22: 324–33.

Hughes AJ, Daniel SE, Kilford L, Lees AJ. Accurancy of clinical diagnosis of idiopathic Parkinson's disease: a cliniopathological study of 100 cases. J Neurol Neurosurg Psychiatry 1992; 55: 181–4.

Innis R, Baldwin R, Sybirska E, Zea Y, Laruelle M, al-Tikriti M, et al. Single photon emission computed tomographic imaging of monoamine reuptake sites in primate brain with [123I]CIT. Eur J Pharmacol 1991; 299: 369–70.

Juh R, Kim J, Moon D, Choe B, Suh T. Different metabolic patterns analysis of Parkinsonism on the 18F-FDG PET. Eur J Radiol 2004; 51: 223–33.

Kojima A, Matsumoto M, Takahashi M, Hirota Y, Yoshida H. Effect of spatial resolution on SPECT quantification values. J Nucl Med 1989; 30: 508–14.

Kuikka JT, Bergstrom KA, Ahonen A, Lansimies E. The dosimetry of iodine-123 labelled 2 beta-carboxymethoxy-3 beta (4-iodophenyl)tropane. Eur J Nucl Med 1994; 21: 53–6.

Laruelle M, Wallace E, Seibyl JP, Baldwin RM, Zea Ponce Y, Zoghbi SS, et al. Graphical, kinetic, and equilibrium analyses of *in vivo* [123I] beta- CIT binding to dopamine transporters in healthy human subjects. J Cereb Blood Flow Metab 1994; 14: 982–94.

Neumeyer JL, Wang SY, Milius RA, Baldwin RM, Zea-Ponce Y, Hoffer PB, et al. [123I]-2β-carbomethoxy-3β-(4-iodophenyl)tropane: high-affinity SPECT radiotracer of monoamine reuptake sites in the brain. J Med Chem 1991; 34: 3144–6.

Papp MI, Lantos PL. The distribution of oligodendroglial inclusions in multiple system atrophy and its relevance to clinical symptomatology. Brain 1994; 117: 235–43.

Pirker W, Asenbaum S, Kasper S, Walter H, Angelberger P, Koch G, et al. β-CIT SPECT demonstrates blockade of 5HT-uptake sites by citalopram in the human brain *in vivo*. J Neural Transm Gen Sect. 1995; 100: 247–56.

Pirker W, Asenbaum S, Bencsits G, Praxer D, Gerschlager W, Deecke L, et al. [123I]beta-CIT SPECT in multiple system atrophy, progressive supranuclear palsy, and corticobasal degeneration. Mov Disord 2000a; 15: 1158–67.

Pirker W, Asenbaum S, Hauk M, Kandlhofer S, Tauscher J, Willeit M, et al. Imaging serotonin and dopamine transporters with iodine-123-beta-CIT-SPECT: binding kinetics and effects of normal aging. J Nucl Med 2000b; 41: 36–44.

Pirker W, Djamshidian S, Asenbaum S, Gerschlager W, Tribl G, Hoffmann M, et al. Progression of dopaminergic degeneration in Parkinson's disease and atypical parkinsonism: a longitudinal beta-CIT SPECT study. Mov Disord 2002; 17: 45–53.

Poewe W, Scherfler C. Role of dopamine transporter imaging in investigation of parkinsonian syndromes in routine clinical practice. Mov Disord 2003; 18: S16–21.

Rakshi JS, Uema T, Ito K, Bailey DL, Morrish PK, Ashburner J, et al. Frontal, midbrain and striatal dopaminergic function in early and advanced Parkinson's disease: a 3D [18F]dopa-PET study. Brain 1999; 122: 1637–50.

Scherfler C, Khan NL, Pavese N, Eunson L, Graham E, Lees AJ, et al. Striatal and cortical pre- and postsynaptic dopaminergic dysfunction in sporadic parkin-linked parkinsonism. Brain 2004; 127: 1332–42.

Schocke MFH, Seppi K, Esterhammer R, Kremser C, Jaschke W, Poewe W, et al. Trace of diffusion tensor differentiates the Parkinson variant of multiple system atrophy and Parkinson's disease. Neuroimage 2004; 21: 1443–51.

Schulz JB, Klockgether T, Petersen D, Jauch M, Mueller-Schauenburg W, Spieker S, Voigt K, Dichgans J. Multiple system atrophy: natural history, MRI morphometry, and dopamine receptor imaging with [123I]IBZM-SPECT. J Neurol Neurosurg Psychiatry 1994; 57: 1047–56.

Schulz JB, Skalej M, Wedekind D, Luft AR, Abele M, Voigt K, et al. Magnetic resonance imaging-based volumetry differentiates idiopathic Parkinson's syndrome from multiple system atrophy and progressive supranuclear palsy. Ann Neurol 1999; 45: 65–74.

Seibyl JP, Marek KL, Quinlan D, Sheff K, Zoghbi S, Zea-Ponce Y, et al. Decreased single-photon emission computed tomographic [123I]beta-CIT striatal uptake correlates with symptom severity in Parkinson's disease. Ann Neurol 1995; 38: 589–98.

Staley JK, Basle M, Flynn DD, Mash DC. Visualizing dopamine and serotonin transporters in the human brain with the potent cocaine analogue [25I]RTI-55: in vitro binding and autoradiographic characterization. J Neurochem 1994; 62: 549–56.

Uhl GR. Neurotransmitter transporter: a promising new gene family. Trends Neurosci 1992; 15: 265–8.

Van Laere K, Santens P, Bosman T, De Reuck J, Mortelmans L, Dieckx R. Statistical parametric mapping of 99mTc-ECD SPECT in idiopathic Parkinson's disease and multiple system atrophy with predominant parkinsonian features: correlation with clinical parameters. J Nucl Med 2004; 45: 933–42.

Varrone A, Marek KL, Jennings D, Innis RB, Seibyl JP. [123I]beta-CIT SPECT imaging demonstrates reduced density of striatal dopamine transporters in Parkinson's disease and multiple system atrophy. Mov Disord 2001; 16: 1023–32.

Wenning GK, Tison F, Ben-Shlomo Y, Daniel SE, Quinn NP. Multiple system atrophy: a review of 203 pathologically proven cases. Mov Disord 1997, 12: 133–47.

Wenning GK, Colosimo C, Geser F, Poewe W. Recent advances in multiple system atrophy. Lancet Neurology 2004; 3: 93–103.

Whone AL, Moore RY, Piccini P, Brooks DJ. Plasticity of the nigropallidal pathway in Parkinson's disease. Ann Neurol 2003; 53: 206–13.